Theor. Appl. Climatol. 54, 85–98 (1996)

Theoretical and Applied Climatology

[1] CSIRO Division of Soils, PMB, PO Aitkenvale, Townsville, Australia
[2] Department of Agronomy, Iowa State University, Ames, Iowa, U.S.A.

Modeling the Impact of Partial Surface Mulch on Soil Heat and Water Flow*

K. L. Bristow[1] and **R. Horton**[2]

With 9 Figures

Received July 1, 1994
Revised February 17, 1995

Summary

Surface residue is an integral part of many cropping systems, and there are opportunities to optimise its value as mulch by improving our understanding of how it affects the near surface soil physical environment. In this study we use field measurements and a coupled soil heat and water flow model to demonstrate the effects of partial surface mulch on the near surface soil physical environment. The model is based on general physical laws and allows analysis of general system behaviour in response to changes in both inputs and systems variables. The field measurements were obtained on both a clay and a sand soil from experiments carried out in the semi-arid tropics. The treatments included a bare soil surface and 0 (completely mulched), 5 cm and 15 cm bare row zones. Both measurements and simulations showed that partial surface mulch cover can have dramatic effects on the soil physical environment near the soil surface, with the development of very strong horizontal gradients across bare soil–mulched soil boundaries. They also show that bare row zones are able to act as either a source or sink for heat and water, and that the resultant soil environmental conditions will exert strong control of soil biological activity. Although model simulations did not always match exactly with the specific measurements, they did capture the major trends given by the field data. While this suggests a certain robustness about the way the processes are modeled, there are several areas in which the model needs improvement and these are highlighted in the paper.

* Journal Paper No. J16277 of the Iowa Agricultural Home Economics Experiment Station, Ames, IA.

1. Introduction

Crop residues which are used as surface mulch are an important feature in many cropping systems where it is now common practice to leave the remains of crops on the field following harvest (McCown et al., 1980; Heilman et al., 1992). Surface mulch can have dramatic effects on the way energy is partitioned at the soil surface, and this can lead to very different rates of drying between mulched and bare soil (Bond and Willis, 1969, 1970; Unger and Parker, 1976; Saxton et al., 1988). Differences in drying rates can in turn lead to very different soil physical conditions (quantified in terms of soil water, temperature and strength) near the soil surface, which then impact on most other soil physical (e.g., runoff, erosion), chemical (e.g., reaction rates), and biological (e.g., seedling establishment, microbial activity) processes. Although there are many situations in which mulch coverage of the soil surface is spatially uniform, this is not always the case. Surface mulch can occur in strips which are separated by areas of bare soil, and this may occur as an indirect consequence of a tillage or planting operation, or it may be done intentionally with a specific management goal in mind (Bristow and Abrecht, 1989; Horton et al., 1994).

A major feature of the system involving alternating strips of mulched and bare soil is the

positional variation of the surface energy balance in the direction perpendicular to the mulched strips, with abrupt changes in the surface energy balance between the bare and mulched soil. Because heat and water move both vertically and horizontally, these abrupt changes in the surface energy balance will not necessarily yield abrupt changes in soil physical conditions. The horizontal differences in soil physical conditions will in fact be damped, and become insignificant at some depth in the soil. The same applies above ground, where horizontal temperature and water gradients decrease with height above the surface due to mixing in the lower atmosphere.

Because near surface physical conditions are affected by the spatial distribution of the surface mulch, opportunities exist for modifying the near surface environment through active management of the surface mulch. There are, however, costs associated with modifying the relationship between mulch covered and bare soil, and the benefits will depend on weather conditions, mulch properties and soil type. Because of the complex interactions between the various components of the soil-mulch-atmosphere system, efforts to identify the best mulch configurations over a range of conditions will therefore need to involve simulation studies as well as field studies (Bristow and Abrecht, 1989). Several past studies have investigated issues associated with surface mulch (Bond and Willis, 1969, 1970; Unger and Parker, 1976; Radke, 1982; Ross et al., 1985; Bristow et al., 1986; Chung and Horton, 1987; Bristow, 1988; Kluitenberg and Horton, 1990; Hares and Novak, 1992a, b), but our understanding of the many complex interactions is still limited (Horton et al., 1994). These latter authors have therefore stressed the need for more effort to be directed to improving the understanding of the near surface physical environment, especially for situations involving partial surface cover. This is essential if we are to improve the management and hence beneficial effects of surface mulch, particularly when limited quantities of mulch material are available.

In this paper we explore the effects of partial surface mulch on the near surface soil physical environment. We use both field measurements and a two-dimensional coupled soil heat and water flow model to do this, and focus specifically on what happens near mulched soil-bare soil boundaries. We use the model to demonstrate the interplay between soil, mulch and atmospheric conditions, and conclude by highlighting areas in need of additional study.

2. The Physical System

The physical system analysed in this study comprises the soil, surface mulch and lower atmosphere. The surface mulch is assumed to occur in parallel strips separated by bare row zones. A schematic of the cross section perpendicular to the row direction and the 2-D grid used in the model described below is given in Fig. 1. Transport of heat and water below the soil surface is treated in two-dimensions, while transport above the soil surface is treated using classical micrometeorological theory for one-dimensional transport in the vertical (Campbell, 1977). The assumption is that there is no horizontal exchange of heat and water between the different surfaces, even though the mulch and bare areas may have very

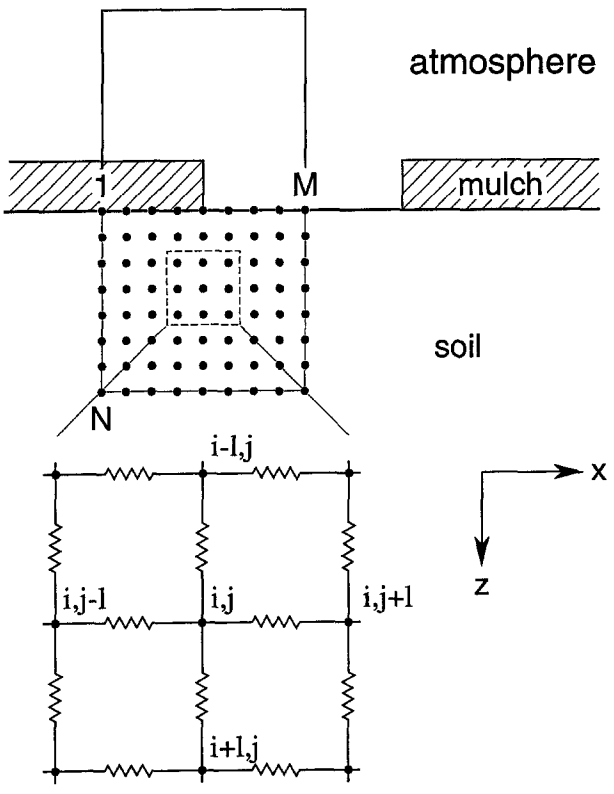

Fig. 1. Schematic of the soil-mulch-atmosphere system showing a cross section perpendicular to the row direction. The flow region is bounded by the solid line and shows the two-dimensional grid used in analysing soil heat and water flow. It also shows an enlarged section with node numbering

different surface properties and hence quite different surface energy balances.

3. The Simulation Model

In this section we summarise the main features of the simulation model used in this study. The model is based on that developed by Chung and Horton (1987), and describes the transport of heat and water within the soil by means of partial differential equations (see Eqs. (1) and (2)). These equations arise by combining the conservation laws for energy and mass with the appropriate flux equations. Estimates of soil temperature and water are obtained using numerical solutions to the governing equations which are applied using an electrical circuit analogy. This involves dividing the system into a number of nodes which are separated by conductance elements, and treating the physical transfer of mass and energy as current flows between nodes. Differences in temperature or water potential at the nodes act as driving forces, and nodes may have capacitance to simulate storage within the system. The above and below ground parts of the system are coupled via the surface energy balance.

3.1 Below Ground Transport

The governing equations for transient soil heat and water flow which make up the heart of the model are based on those developed by Philip and De Vries (1957), which in two-dimensions are written as

$$\rho c \frac{\partial T}{\partial t} = \frac{\partial}{\partial x}\left[k_t \frac{\partial T}{\partial x}\right] + \frac{\partial}{\partial z}\left[k_t \frac{\partial T}{\partial z}\right] + S(x,z,t) \qquad (1)$$

and

$$C_w \frac{\partial \psi}{\partial t} = \frac{\partial}{\partial x}\left[k_w \frac{\partial \psi}{\partial x}\right] + \frac{\partial}{\partial z}\left[k_w\left(\frac{\partial \psi}{\partial z} + 1\right)\right] + Q(x,z,t) \qquad (2)$$

for heat and water flow, respectively. Here ρc is soil volumetric heat capacity ($J\,m^{-3}\,K^{-1}$), T is temperature (°C), t is time (s), x is horizontal distance (m), k_t is thermal conductivity ($W\,m^{-1}\,K^{-1}$), z is vertical distance (m), S is a source/sink term for heat energy ($J\,m^{-3}\,s^{-1}$), C_w is water capacity specified by the slope of the soil water retention curve (m^{-1}), ψ is soil matric potential (m), k_w is hydraulic conductivity ($m\,s^{-1}$), and Q is a source/sink term for water (s^{-1}).

The key soil physical properties needed to solve Eqs. (1) and (2) are the storage and transmission properties, which define the volumetric heat capacity and thermal conductivity for heat, and the soil water retention and hydraulic conductivity for water. The actual equations used in the current model are

$$\rho c = 1.92 \times 10^6 \phi_s + 2.51 \times 10^6 \phi_0 + 4.18 \times 10^6 \theta \qquad (3)$$

for the volumetric heat capacity (de Vries, 1963), where ϕ_s is the volume fraction of solids, ϕ_0 is the volume fraction of organic matter, and θ is the volumetric water content. Thermal conductivity is expressed as a function of water content as (Campbell, 1985)

$$k_t = A + B\theta - (A - D)\exp(-(C\theta)^4) \qquad (4)$$

where $A = 0.65 - 0.78\rho_b + 0.60\rho_b^2$, $B = 1.06\rho_b$, $C = 1 + 2\phi_c^{-1/2}$, $D = 0.03 + 0.7(1 - \theta_s)^2$, ρ_b is bulk density, ϕ_c is volume fraction of clay, and θ_s is the saturated volumetric water content.

Functions developed by van Genuchten (1980) are used to describe the soil water retention curve

$$\theta = \theta_r + (\theta_s - \theta_r)\left[\frac{1}{1 + (\alpha\psi)^n}\right]^{1 - 1/n} \qquad (5)$$

and soil hydraulic conductivity function

$$k_w = k_s \Theta^{1/2}[1 - (1 - \Theta^{1/m})^m]^2. \qquad (6)$$

Here, θ_r is the residual volumetric water content, α and n are empirical coefficients, ψ is matric potential, Θ is the fractional water content defined as $(\theta - \theta_r)/(\theta_s - \theta_r)$, and $m = 1 - 1/n$. The water capacity C_w is obtained by writing Eq. (5) in terms of ψ and taking the derivative $\partial\psi/\partial\theta$.

Other water content dependent soil properties required in the model are the soil emissivity ε_s and soil surface albedo α_s. The equations used are based on those of van Bavel and Hillel (1976), expressed as

$$\varepsilon_s = 0.9 + 0.18\theta \qquad (7)$$

and

$$\begin{aligned} \alpha_s &= 0.25 && \theta \leqslant 0.10 \\ \alpha_s &= 0.35 - \theta && 0.10 \leqslant \theta \leqslant 0.25 \\ \alpha_s &= 0.10 && \theta \geqslant 0.25 \end{aligned} \qquad (8)$$

Subsurface vapor flow has been added to the model by determining the thickness of the 'dry

layer' at the soil surface, and calculating vapor flow through this layer using Fick's law diffusion calculations. The vapor flow calculated in this way is then added to liquid flow in this 'dry layer' to give total water flow. For the simulations carried out in this study 'dry soil' was defined as that soil that was less than 50% saturated. Thermally induced liquid flow is considered negligibly small (Jackson et al., 1974) and is not included in this model.

Solution of Eqs. (1) and (2) to obtain soil temperature and water as a function of time and position within the two-dimensional grid (Fig. 1) is achieved using numerical methods. The actual procedure involves the Alternating-Direction Implicit (ADI) scheme (Lapidus and Pinder, 1982) to solve finite difference approximations of Eqs. (1) and (2). The solution is initiated by specifying system properties and initial values of each variable for each node in the flow region at the beginning of the simulation. Boundary conditions are derived from input data, and involve value specified boundary conditions at the top (i.e. at the soil surface) and bottom boundary for heat flow, no-flow boundary conditions for the left and right boundaries for both heat and water flow, and flux boundary conditions for top and bottom boundaries for water flow. The top boundary conditions are not known explicitly but are determined as part of the overall solution process in which the surface energy balance is used to couple above and below ground components. Additional details of the numerical methods and solution procedure are given by Chung and Horton (1987).

3.2 Above Ground Transport

In the current model above ground transport is treated using classical micrometeorological theory (Campbell, 1977), with transport above and below ground being linked through the surface energy balance. For bare soil the surface energy balance is written as

$$R_n = LE + H + G \tag{9}$$

where R_n is net radiation ($W\,m^{-2}$), LE is latent heat flux density ($W\,m^{-2}$), H is sensible heat flux density ($W\,m^{-2}$), and G is soil heat flux density ($W\,m^{-2}$). Net radiation is determined as

$$R_n = (1 - \alpha_s)S_t + L_i - L_0 \tag{10}$$

where α_s is the surface albedo, S_t is incoming shortwave radiation ($W\,m^{-2}$), L_i is longwave sky irradiance ($W\,m^{-2}$), and L_0 is longwave radiation emitted by the surface ($W\,m^{-2}$). The longwave components are determined using Stefan-Boltzman type equations written in the form (van Bavel and Hillel, 1976)

$$L = \sigma\varepsilon T^4 \tag{11}$$

where σ is the Stefan-Boltzman constant ($5.67 \times 10^{-8}\,W\,m^{-2}\,K^{-4}$), ε is emissivity of the surface (or atmosphere), and T is temperature of the surface (or atmosphere) expressed in degrees Kelvin.

The latent and sensible heat fluxes are calculated as

$$LE = L(\rho_{vs} - \rho_{va})/r_{va} \tag{12}$$

$$\text{with} \quad L = 2.49463 \times 10^9 - 2.247 \times 10^6 T_s, \tag{13}$$

and

$$H = \rho c_p (T_s - T_a)/r_{ha} \tag{14}$$

where L is latent heat of vaporization ($J\,kg^{-1}$), ρ_{vs} is vapor density at the surface ($kg\,m^{-3}$), ρ_{va} is atmospheric vapor density ($kg\,m^{-3}$), r_{va} and r_{ha} are the aerodynamic resistances ($s\,m^{-1}$) to vapor and heat transport, respectively, and ρc_p is air volumetric heat capacity ($J\,m^{-3}\,K^{-1}$). The surface vapor density is calculated using the Kelvin equation

$$\rho_{vs} = \rho_{vs}^* \exp[(M_w g\psi)/(RT_s)] \tag{15}$$

where ρ_{vs}^* is the saturated vapor density ($kg\,m^{-3}$), M_w is molecular weight of water ($kg\,mole^{-1}$), g is acceleration due to gravity ($9.8\,m\,s^{-2}$), ψ is matric potential (m) at the surface, R is the universal gas constant ($8.314\,J\,mole^{-1}\,K^{-1}$), and T_s is surface temperature (K).

The aerodynamic boundary layer resistances are functions of wind speed and surface structure and are calculated as (van Bavel and Hillel, 1976)

$$r_{va} = r_{ha} = [\ln(z/z_0)]^2/(0.16u) \tag{16}$$

where z_0 is the roughness length (m), z is height (m), and u is wind speed ($m\,s^{-1}$).

The soil heat flux density at the soil surface is determined using a modified form of Fourier's law of heat conduction as described by Chung and Horton (1987).

In this model the mulch layer is treated as a nontransparent cover so that radiation does not

penetrate the mulch (Chung and Horton, 1987). This requires that separate surface energy balances be determined for the mulch-atmosphere interface and for the mulch-soil interface. The energy balance at the mulch-atmosphere interface is determined as

$$R_n = H + M \tag{17}$$

where R_n and H are as determined previously, except that the surface is now the mulch surface and not the soil surface. M is the heat flux density through the mulch ($W\,m^{-2}$) and is determined as

$$M = k_m(T_m - T_s)/\Delta m \tag{18}$$

where k_m is the thermal conductivity of the surface mulch ($W\,m^{-1}\,K^{-1}$), T_m is the temperature of the mulch surface (°C), and Δm is the thickness of the mulch layer. For the mulch-soil interface the energy equation is

$$M = LE + G \tag{19}$$

where the latent heat flux density is now calculated as

$$LE = L(\rho_{vs} - \rho_{va})/(r_{va} + r_{vm}) \tag{20}$$

and r_{vm} is an additional resistance term to account for vapor transport through the mulch layer. This resistance term is determined as (van Bavel and Hillel, 1976)

$$r_{vm} = \Delta m/(D_a f \tau) \tag{21}$$

where D_a is vapor diffusivity in air ($m^2\,s^{-1}$), f is porosity of the mulch, and τ is tortuosity.

An iterative procedure (the bisection method) is used to solve Eqs. (9) and (19) for surface temperature T_s, which then facilitates determination of all surface energy balance components. Additional details of the solution procedure are given by Chung and Horton (1987).

4. Field Data

Measured data used in this study were obtained from a field experiment carried out in the semi-arid tropics at Katherine in the Northern Territory, Australia (14° 28′ S, 132° 18′ E, 108 m altitude) over an 8 day period in April 1986. Details of both the experimental set up and data analysis are given by Bristow and Abrecht (1989) and Abrecht and Bristow (1990).

Two soil types, a sand (paleustalf) and clay (oxic paleustalf), were available at the study site. Soil physical properties determined using standard soil physical procedures (Klute, 1986) are summarised in Table 1. Analyses to determine soil hydraulic properties were carried out on undisturbed soil cores (7.5 cm diameter by 5 cm deep). Coconut fibre matting was used as the surface mulch in this experiment to obtain sharp boundaries between the bare and mulched soil. The mulch was positioned to give north/south oriented bare row zones of 0 (fully mulched), 5 cm,

Table 1. *Summary of Soil Physical and Surface Mulch Properties*

Physical property*	Sand	Clay	Mulch
% sand	92	49	n/a
% silt	2	15	n/a
% clay	6	36	n/a
ρ_b ($Mg\,m^{-3}$)	1.50	1.43	n/a
θ_s($m^3\,m^{-3}$)	0.436	0.462	n/a
k_s($m\,s^{-1}$)	3.206×10^{-4}	3.588×10^{-6}	n/a
α	500	45	n/a
n	1.22	1.09	n/a
ϕ_s	0.564	0.538	n/a
ϕ_{om}	0	0	n/a
z_0(m)	0.005	0.010	0.010
Δm(m)	n/a	n/a	0.012
α_s	Eq. (8)	Eq. (8)	0.40
k($W\,m^{-1}\,K^{-1}$)	Eq. (4)	Eq. (4)	0.125

* ρb = bulk density; θ_s = saturated water content; k_s = saturated conductivity; α and n = coefficients in the van Genuchten hydraulic property function; ϕ_s = fraction of solid material; ϕ_{om} = fraction of organic matter; z_0 = surface roughness; Δm = thickness; α_s = surface albedo; k = thermal conductivity; n/a = not applicable.

Table 2. *Environmental Data* Measured During the Experimental Period*

Day	S_t (MJ m^{-2})	T_{max} (°C)	T_{min} (°C)	u (m s^{-1})	E_p (mm)
1	22.1	34.1	19.2	0.21	4.3
2	23.8	34.6	20.6	0.36	4.4
3	21.4	34.0	20.3	0.31	5.6
4	23.3	35.0	19.2	0.65	5.6
5	24.1	35.2	18.9	.055	5.8
6	25.6	35.3	14.3	0.49	6.5
7	23.4	34.9	11.5	0.30	6.7
8	24.1	34.2	12.8	0.66	5.3

* S_t = solar irradiation; T_{max} and T_{min} = maximum and minimum air temperature; u = average wind speed; E_p = pan evaporation.

and 15 cm width. A completely bare soil treatment was also included. The mulch properties are included in Table 1.

The whole experimental site was irrigated following instrument installation. This allowed differences in drying behaviour between the bare and mulched zones to be studied as the system dried. Environmental variables including incoming solar radiation, maximum and minimum air temperature, wind speed, and pan evaporation were measured throughout the experiment (Table 2). No rain occurred during this period. Measurements of net radiation, soil water and soil temperature were also obtained in selected plots as a function of time as described by Bristow and Abrecht (1989).

5. Simulation Runs

A rectangular grid (0.25 m × 0.25 m) with uniform soil properties was used to represent the two-dimensional soil zone for the simulations discussed here. The origin is taken as the upper left corner, with x horizontal to the right (nodes 1 to M) and z vertically down (nodes 1 to N) (Fig. 1). Because of symmetry, this one section is sufficient to describe the alternating bare/mulched system we were dealing with. We used a spatial step size of 0.025 m in the simulations and a time step that never exceeded 300 s.

Soil, mulch and environmental data used as inputs for the simulation runs were based on the measurements made at katherine (Tables 1, 2). Empirical expressions employing sine functions were used to impose diurnal trends in solar radiation, air temperature, and wind speed. The minimum and maximum air temperatures were set to occur at 3 am and 3 pm. Atmospheric vapor density was calculated as the saturated vapor density at the minimum measured air temperature (Bristow, 1992).

Simulation runs were carried out for the bare soil and 0 (fully mulched), 5 and 15 cm bare row zone treatments for both the sand and clay soils. Some comparisons are made between the two soils, but most discussion is focussed on the 15 cm bare row zone treatment on the clay soil. Conditions at nodes 1 and M in the x direction are highlighted. These nodes represent conditions under full mulch and in the middle of the bare row zone, respectively (Fig. 1). Contour plots which show the temperature and water distribution across the bare soil – mulched soil boundary are included. Comparisons with available field data are also included.

6. Results and Discussion

6.1 Surface Energy Balance

Figure 2 illustrates the cumulative (Σ) value of each component of the surface energy balance for the 15 cm bare row treatment on the clay soil over the 8 day simulation period. Values for node 1 under the mulch and node M at the centre of the bare row are compared. The diurnal variation in all components is obvious. ΣR_n in the bare row zone showed a steady increase, averaging about 12 MJ m^{-2} d^{-1}. ΣR_n under mulch also showed a steady increase but averaged only about 6 MJ m^{-2} d^{-1}.

There was a rapid increase in ΣLE during the first two days in the bare row and then a gradual reduction in the rate of increase thereafter. This reflects the high evaporation under wet condi-

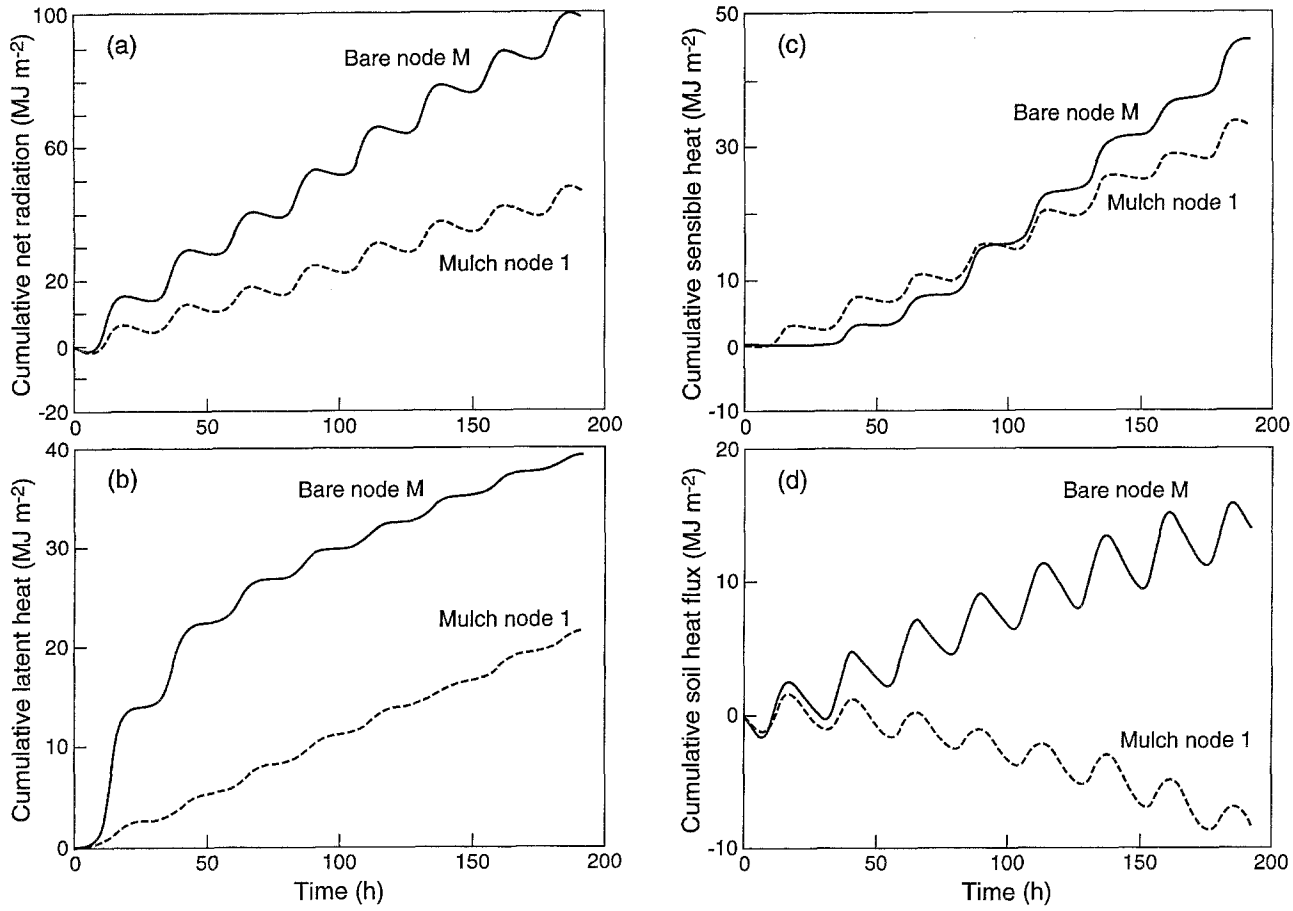

Fig. 2. Simulated energy balance components for the soil showing (a) net radiation (b) latent heat flux density (c) sensible heat flux density and (d) soil heat flux density. These are cumulative values for the 8 day simulation period for the 15 cm bare row zone treatment. Node 1 represents mulched conditions and node M the middle of the bare row

tions ($LE = 14\,\mathrm{MJ\,m^{-2}}$ on day 1) and a rapid reduction in evaporative loss as the near surface dried to very low values by the end of the 8 day period ($LE = 1.8\,\mathrm{MJ\,m^{-2}}$ on day 8). The mulched soil showed a steady increase in ΣLE throughout the experimental period, averaging roughly $2.5\,\mathrm{MJ\,m^{-2}\,d^{-1}}$. This indicates maintenance of relatively wet conditions near the soil surface under the mulch and strong control of water loss by the surface mulch.

Sensible heat loss from the mulched surface was low the first day when conditions were wet, but then remained fairly constant for the remainder of the simulation period, averaging roughly $4\,\mathrm{MJ\,m^{-2}\,d^{-1}}$. Sensible heat flux in the bare row was also low initially, but increased significantly as the bare row dried, exceeding that lost from the mulched soil by day 5. These results again reflect changes in the moisture status of the system with sensible heat loss increasing as latent heat loss decreases.

Daily total soil heat flux density in the bare row was less than 10% of incoming shortwave radiation on all days except one, and showed a net input of heat energy to the soil over the 8 day period. This was reversed in the case of the mulched soil which showed a net loss of energy from the soil during this period (Fig. 2d). This suggests that some of the energy entering the soil at the bare row moved out horizontally under the mulch, a hypothesis supported by the temperature data discussed in a later section which shows strong horizontal gradients across the bare soil – mulched soil boundary. Given these results, one can visualise the bare row acting as a kind of 'heat pump' during the day, drawing energy into the system at the bare row and cycling it out from under the mulch back to the atmosphere.

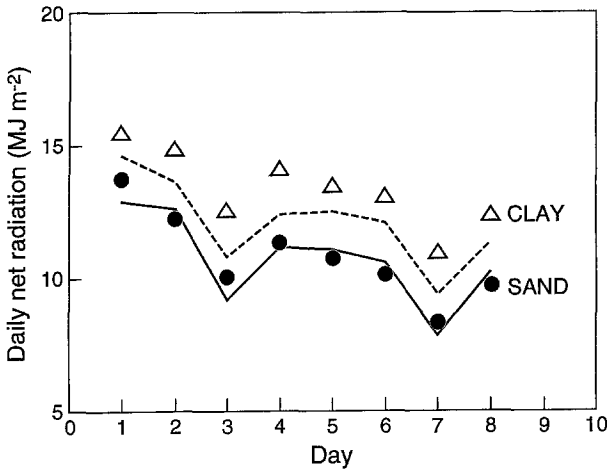

Fig. 3. Comparison of measured (points) and simulated (lines) daily net radiation for the bare soil treatments on both the clay (Δ, ------) and sand (●, ——)

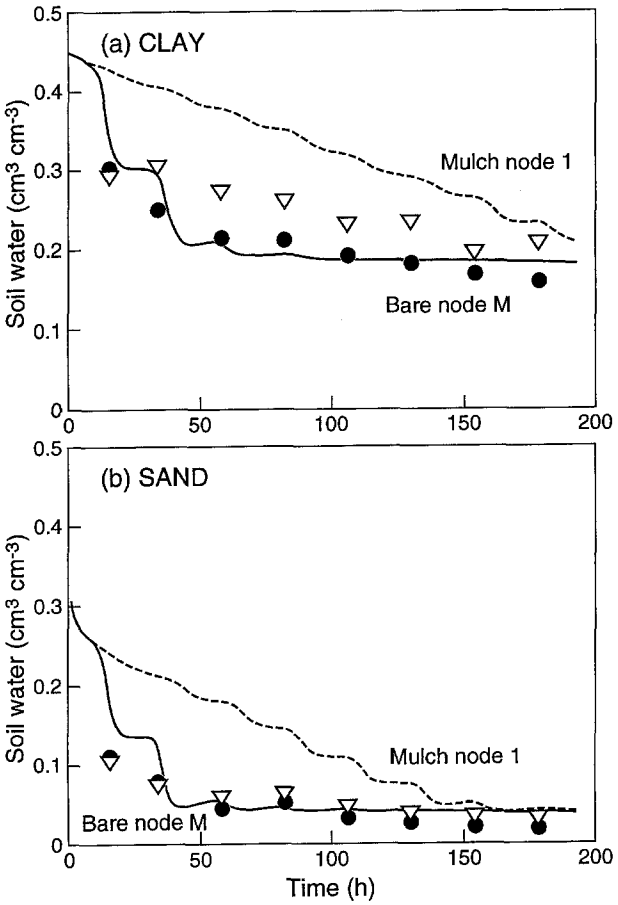

Fig. 4. Soil water as a function of time for the 15 cm bare row treatment on the (a) clay and (b) sand. Points (∇ mulched; ● bare) are measurements for the 0–5 cm layer, and lines are simulated values at 2.5 cm depth

Comparison of measured and simulated net radiation for the completely bare treatments is shown in Fig. 3. Agreement between simulated and measured values is good in the case of the sand, but not particularly good for the clay. The simulated values do however follow the measured trends, and although the offset in actual values may imply that the instruments were in error, it is more likely that the system properties used in the simulations don't quite match with those that existed in the field.

6.2 Soil Water

It is clear from the latent heat data (Fig. 2b) that high rates of water loss occurred on days 1 and 2 from the bare row zone in both soils, and this is reflected by the water content data given in Fig. 4. The simulated data are for the 2.5 cm deep node and show a rapid decrease in water content in the bare row zone over the first two days, and apart from small diurnal variations, essentially no change thereafter. There was a slow steady loss of water from under the mulch, with the water content at this node approaching that of the bare row by the end of the 8 day period. These water content data also show diurnal trends which reflect the greater loss of water during the day under high evaporative demand conditions, with some replenishment of water from deeper in the profile at night under lower evaporative demand conditions.

Field measured water contents of the 0–5 cm surface layer are included in Fig. 4 for comparative purposes. These data (obtained using 25 mm diameter cores) obviously cannot provide the same level of detail as the simulated data which show conditions at a point in the profile. They do however show reasonably good agreement with the simulated values for the bare row zones, where most of the water content change occurred in the first two days, with very little change thereafter. Although measurements yielded higher water contents for the mulched soil than for the bare soil, the agreement with simulated values under mulch is poor.

Contour plots of simulated water content at 1400 h on day 3 are shown in Fig. 5 for the 15 cm bare row treatment for both the sand and clay. Water contents are lowest in the upper right hand corner indicating that soil in the bare row zone

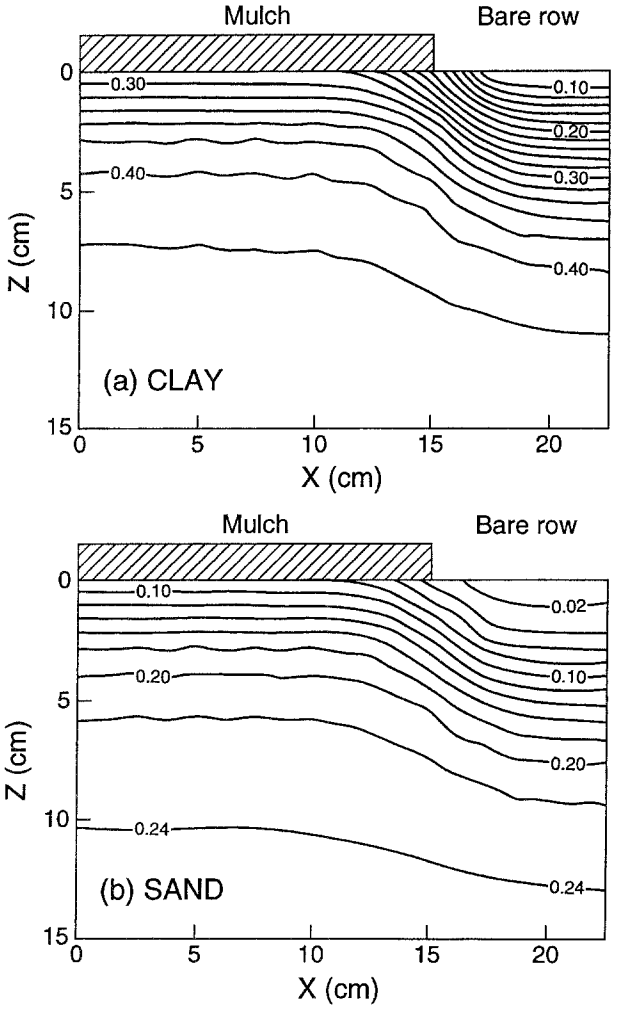

Fig. 5. Contour plots of soil water contents for the 15 cm bare row treatment at 1400 h on day 3 for the (a) clay and (b) sand

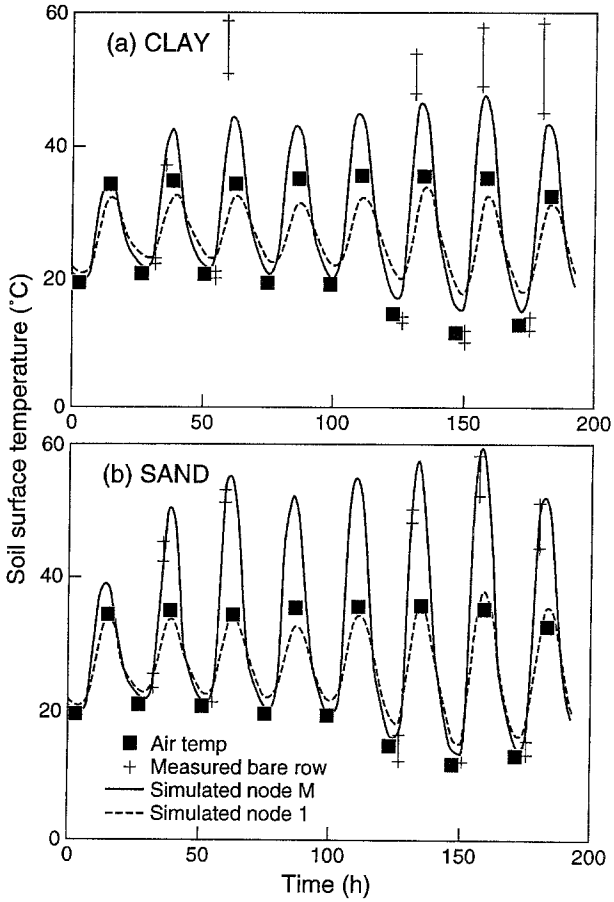

Fig. 6. Diurnal variation in soil surface temperature for the 15 cm bare row treatment for the 8 day experimental period for the (a) clay and (b) sand. The range in measured surface temperature in the bare row is shown by the vertical lines

has lost much more water than the soil under the mulch. The high density of contour lines in the upper right hand corner also show that there are very strong vertical and horizontal gradients in this region, and that water would be pulled from depth and from beneath the mulch. The horizontal gradients do decrease with depth and become negligible by about 10–15 cm depth.

6.3 Soil Temperature

Simulated temperature at the soil surface as a function of time under the mulch (node 1) and in the middle of the bare row (node M) for the 15 cm bare row treatment is shown in Fig. 6 for the clay and sand. There is not much difference in temperature between the mulched and bare areas on the first day when conditions were wet, but by the second day significant differences had developed with the bare soil temperatures showing much greater extremes than the mulched soil. Surface temperatures of the bare row measured using a handheld infrared thermometer are also included, and show very high values (up to 60 °C) during the day once the surface soil had dried. Simulated values agreed well with measurements on the sand, but underestimated the high daytime temperature on the clay. Measured maximum and minimum air temperatures are also included in Fig. 6. They show that the temperature extremes of the soil surface under the mulch were within 5 °C of the air temperature extremes throughout the 8 day period except for the last 3 days when the presence of a cooler air mass resulted in signifi-

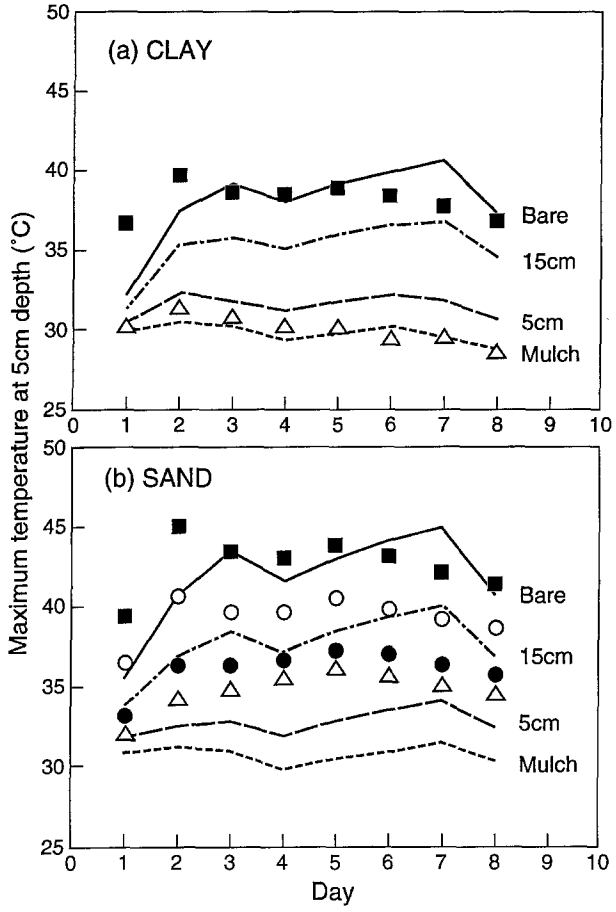

Fig. 7. Maximum soil temperature at 5 cm depth in the bare soil treatment (■) and at the centre of the 0 (completely mulched, Δ), 5 (●) and 15 cm (○) bare row zones for the (a) clay and (b) sand. Points are measured data and lines are simulated data

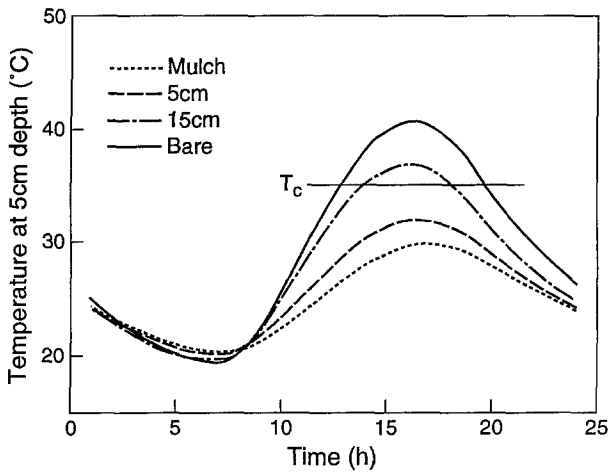

Fig. 8. Variation in simulated temperature at 5 cm depth in the bare treatment and at the centre of the 15 cm, 5 cm, and 0 cm (completely mulched) bare row zones for the clay. T_c shows the 35 °C temperature

cantly lower minimum air temperatures than were experienced on the first few days.

Maximum temperature at 5 cm depth in the middle of the 0 (completely mulched), 5 and 15 cm wide bare row zones and in the middle of the bare treatment are shown in Fig. 7 for the clay and sand. The points are measured data and the lines simulated data. In general there is an increase in maximum temperature on day 2 as initial drying took place, and then little change, or a gradual decrease in maximum temperature with time. Agreement between measurements and simulations for the clay is reasonable, particularly for the mulched treatment. Agreement is also reasonable for the bare treatment in the sand, but then gets worse for the 15, 5 and 0 cm bare row treatments. Other discrepancies between measured and simulated data exist on day 1 and 7. On day 1 simulations for both the sand and clay show reasonably small differences in temperature between treatments as would be expected under wet conditions. Measurements, however, show much greater differences, up to 8 °C differences between treatments on the sand. Reasons for these large differences between treatments under wet conditions are not clear, as Bristow (1988) showed that it took only a light rain of 6 mm to cause convergence of near surface temperatures under a range of surface mulch treatments. Similarly, the anomaly on day 7 where simulations show an upward spike while measured data show a downward trend is difficult to explain.

The variation in simulated temperature on day 7 at a depth of 5 cm in the bare soil treatment and in the middle of the 15, 5, and 0 cm (completely mulched) wide bare rows is shown in Fig. 8 for the clay soil. These data show that the greatest variation in temperature occurred in the completely bare treatment and that as the bare row width decreased, variation in the thermal environment decreased as expected. These data also highlight the time spent each day above a certain temperature, which can be critical for many biological processes (Bristow and Abrecht, 1991). In the bare treatment, temperatures at 5 cm depth exceeded 35 °C for more than 6 hours, while in the 15 cm treatment it exceeded 35 °C for only 4 hours. Temperature in the 5 cm and completely mulched treatments never exceeded 35 °C. It is clear there-

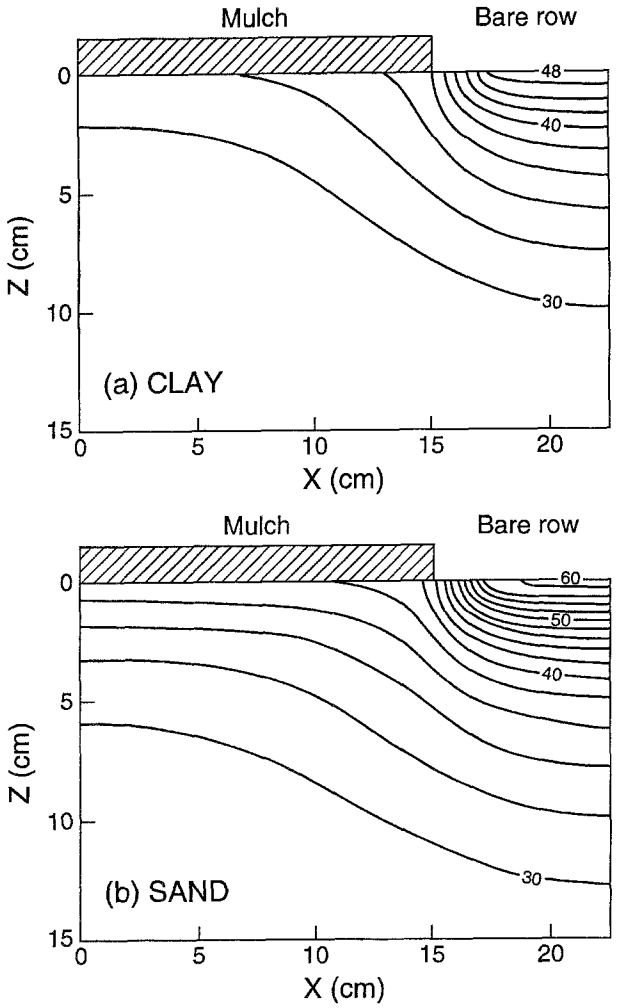

Fig. 9. Contour plots of soil temperature for the 15 cm bare row treatment at 1400 h on day 7 for the (a) clay and (b) sand

fore that near surface temperatures can be controlled by managing the width of the bare row zone.

Contour plots of simulated temperature at 1400 h on day 7 across the boundary between the bare and mulched soil for the clay and sand are shown in Fig. 9. Here we see very high temperatures in the upper right hand corner (middle of the bare row zone), 60 °C in the case of the sand, with strong temperature gradients in the vertical and horizontal directions. A 20 °C change in temperature in less than 10 cm at the surface is a significant gradient (200 K m^{-1}), which will derive heat energy from the bare row zone into the mulch covered soil, thereby increasing water loss from those areas. This spatial variation in temperature will also no doubt have interesting implications in terms of biological activity. As an example, the success of seedling establishment in these types of systems will depend to a large extent on where the seed is placed relative to the mulch soil – bare soil boundary (Abrecht and Bristow, 1989).

6.4 System Property Variation

Models of the type presented here require input of a range of different system properties and have to deal with many interacting processes. There is a need to continue testing these models and evaluating their performance under a wide range of conditions representative of those under which they will be applied. One way to do this is to compare simulations with field measured data as has been done in this study and to carry out sensitivity analyses to determine the relative importance of the various input parameters. These analyses are not trivial when dealing with so many complex, interacting processes, and often require special techniques (Binley et al., 1991; Chaves and Nearing, 1991).

In this paper we choose just one parameter, the soil surface roughness z_0, and demonstrate the sensitivity of model output to changes in z_0. Surface roughness was varied from 0.015 m to 0.005 m for the clay soil in the 15 cm bare row treatment. Results are shown in Table 3, which summarises the cumulative energy balance components, and 0 (surface) and 5 cm deep temperatures in the centre of the bare row zone. There was not much difference in net radiation or latent heat flux, but there were significant changes in partitioning of energy between sensible heat flux and soil heat flux. As z_0 decreased, sensible heat flux decreased, soil heat flux increased, and soil temperatures in the bare row zone increased significantly. These increases, being at the high end of the temperature scale for many biological processes (such as seedling establishment), could play a crucial role in biological performance. They also demonstrate the sensitivity of the model to changes in z_0, which suggests that either z_0 is not being incorporated correctly into the model, or that the effects are real, and that there are real management options available by adjusting the surface roughness. Other model parameters need to be investigated similarly.

7. General Discussion and Conclusions

It is clear from the results of this study that partial surface mulch cover can have dramatic effects on

Table 3. *Effect of Changes in Soil Surface Roughness (z_0) in the 15 cm Bare Row Treatment on cumulative Surface Energy Balance Components* ($MJ\,m^{-2}$) *and Soil Temperature* ($°C$)

z_0 (m)	Node	ΣR_n	ΣLE	ΣH	ΣG	Day 8 T_{max} (0 cm)	Day 8 T_{min} (5 cm)
0.015	1 (mulch)	46.0	21.5	32.6	−8.0	31.2	29.8
	M (bare)	101.5	38.8	52.7	10.0	40.9	33.6
0.010	1 (mulch)	45.9	21.6	32.8	−8.4	31.3	29.9
	M (bare)	98.7	39.2	45.6	13.9	43.2	34.6
0.005	1 (mulch)	45.8	21.7	33.1	−9.0	31.4	30.2
	M (bare)	94.8	39.8	34.9	19.9	46.1	36.1

the soil physical environment near the soil surface. A major feature of partial mulch cover is the positional variation in the surface energy balance and the very strong horizontal gradients that can develop between mulched and bare areas. Bare areas can therefore act as a 'sink' for water, drying out rapidly and drawing water from deeper in the profile and from the mulched areas. Similarly, as the bare row zones dry and get hotter than the surrounding soil, they can act as a heat source for nearby mulched areas and increase the evaporative loss from the mulched areas.

It is also clear from the simulations presented here that the model used in this study captured the trends given by the field data, but that the simulations did not always agree exactly with the measurements (Figs. 3, 4, 6, 7). Some of the discrepancy may reflect a 'mismatch' between properties used in the model and those that existed in the field, and obtaining physically meaningful system properties that accurately reflect field conditions remains a major challenge in testing and validating physically based models like the one used in this study. We however feel that the agreement between simulations and measurements is reasonable given the assumptions (e.g., the nontransparent nature of the mulch) on which the model is based, and the relatively coarse characterisation of the system properties and input data used in the model. There may also be limitations (errors/uncertainties) in the measurements, and not all of the difference between measured and simulated data can be atrributed to limitations in the model. Agreement between measurements and simulations could no doubt have been improved by adjusting, or 'fitting' the parameters, but that was not the purpose of this study. Rather, the aim was to see how well the system could be represented using readily available soil, mulch and weather data in a physically based model, and to use the model to learn more about system behaviour.

Based on our experiences in working with this model and other similar models that are being used to address issues involving surface mulch, there are still several areas that need improvement. There is a need for improved above ground subroutines that can deal with transport through the mulch in a much more realistic way. We know that surface mulch is not nontransparent to radiation, and more realistic radiation exchange algorithms need to be incorporated into these type of models (Shen and Tanner, 1990; Tanner and Shen, 1990a). Improvement in dealing with vapor flow through surface mulches is also needed (Tanner and Shen, 1990b), and the ability to handle condensation of water onto and evaporation of water from surface mulch needs to be included (Bristow et al., 1986). The above ground horizontal transfer of heat and water between the bare and mulched areas can also be significant (Ham et al., 1991), and needs to be addressed if we are to truly understand how these spatially variable systems really work.

There is also a need for improved characterisation and parameterisation of the mulch and soil properties, and particularly their spatial distribution in these nonuniform systems. Simple and practical procedures are needed for obtaining these data. Vapor flow was omitted in the original Chung and Horton (1987) model, and its addition here has improved model performance, particularly in generating more realistic shapes in the near surface water content profiles and more real-

istic changes in variables (e.g., water content, latent heat flux, temperature, soil heat flux) associated with soil drying. There is however still room for improvement on the currently employed simplification and some of the more rigorously based procedures (Bristow et al., 1986) need to be adopted.

There are real strengths in pursuing development of physically based models like the one used in this study, and we encourage greater efforts to be directed this way. We think that the focus should be on models that employ general physical laws that accurately describe the transport processes, and that if there is to be any simplification, then it should take place in the characterisation and parameterisation of the system properties. With this approach, future developments will not require rebuilding of fundamentals, but will enable us to move forward from a solid foundation, resulting in more accurate and widely applicable models (Williams et al., 1991). We need models that provide insight into the interactions within a system, and which allow the implications of various management strategies to be explored. There are many complex interactions between the soil, mulch and atmosphere, and experimental work will always be a restricted subset of possible outcomes. It is imperative therefore that we strive to develop a set of physically based models that will help deal with site and season variations, and allow us to improve our understanding and management of surface mulch.

References

Abrecht, D. G., Bristow, K. L., 1990: Maize seedling response to the soil environment at varying distances from a mulched soil-bare soil boundary. *Soil Tillage Res.*, **15**, 205–216.

Binley, A. M., Bevan, K. J., Calver, A., Watts, L. G., 1991: Changing responses in hydrology: Assessing the uncertainty in physically based model predictions. *Water Resources Res.*, **27**, 1253–1261.

Bond, J. J., Willis, W. O., 1969: Soil water evaporation: Surface residue rate and placement effects. *Soil Sci. Soc. Amer. Proc.*, **33**, 445–448.

Bond, J. J., Willis, W. O., 1970: Soil water evaporation: First stage drying as influenced by surface residue and evaporation potential. *Soil Sci. Soc. Amer. Proc.*, **34**, 924–928.

Bristow, K. L., 1988: The role of mulch and its architecture in modifying soil temperature. *Aust. J. Soil Res.*, **26**, 269–280.

Bristow, K. L., 1992: Prediction of daily mean vapor density from daily minimum air temperature. *Agric. Forest Meteor.*, **59**, 309–317.

Bristow, K. L., Abrecht, D. G., 1989: The physical environment of two semi-arid tropical soils with partial surface mulch cover. *Aust. J. Soil Res.*, **27**, 577–587

Bristow, K. L., Abrecht, D. G., 1991: Daily temperature extremes as an indicator of high temperature stress. *Aust. J. Soil Res.*, **29**, 377–385.

Bristow, K. L., Campbell, G. S., Papendick, R. I., Elliott, L. F., 1986: Simulation of heat and moisture transfer through a surface residue-soil system. *Agric. Forest Meteor.*, **36**, 193–214.

Campbell, G. S., 1977: *An Introduction to Environmental Biophysics.* New York: Springer 159 pp.

Campbell, G. S., 1985: *Soil Physics with BASIC–Transport Models for Soil-plant Systems.* New York: Elsevier, 150 pp.

Chaves, H. M. L., Nearing, M. A., 1991: Uncertainty analysis of the WEPP soil erosion model. *Trans. Amer. Soc. Agric. Eng.*, **34**, 2437–2444.

de Vries, D. A., 1963: Thermal properties of soils. In: van Wijk, W. R., (ed.) *Physics of Plant Environment,* Amsterdam: North Holland, pp. 210–235.

Chung, S. O., Horton, R., 1987: Soil heat and water flow with a partial surface mulch. *Water Resources Res.*, **23**, 2175–2186.

Ham, J. M., Heilman, J. L., Lascano, R. J., 1991: Soil and canopy energy balances of a new crop at partial cover. *Agron. J.*, **83**, 744–753.

Hares, M. A., Novak, M. D., 1992a: Simulation of surface energy balance and soil temperature under strip tillage I Model description. *Soil Sci. Soc. Amer. J.*, **56**, 22–29.

Hares, M. A., Navak, M. D., 1992b: Simulation of surface energy balance and soil temperature under strip tillage II Field test. *Soil Sci. Soc. Amer. J.*, **56**, 29–36.

Heilman, J. L., McInnes, K. J., Gesch, R. W., Lascano, R. J., 1992: Evaporation from ridge-tilled soil covered with herbicide-killed winter wheat. *Soil Sci. Soc. Amer. J.*, **56**, 1278–1286.

Horton, R., Kluitenberg, G. J., Bristow, K. L., 1994: Surface crop residue effects on the soil surface energy balance. In: Unger, P. W. (ed.), *Managing Agricultural Residues.* Boca Raton: Lewis Publishers, pp. 143–162.

Jackson, R. D., Reginato, R. J., Kimball, B. A., Nakayama, F. S., 1974: Diurnal soil water evaporation: comparison of measured and calculated soil water fluxes. *Soil Sci. Soc. Amer. Proc.*, **38**, 861–866.

Kluitenberg, G. J., Horton, R., 1990: Analytical solution for two-dimensional heat conduction beneath a partial surface mulch. *Soil Sci. Soc. Amer. J.*, **54**, 1197–1206.

Klute, A. (ed.), 1986: *Methods of Soil Analysis, Part I Physical and Mineralogical Methods,* 2nd edn. Agronomy 9, American Society of Agronomy, Madison.

Lapidus, L., Pinder, G. F., 1982: *Numerical Solution of Partial Differential Equations in Science and Engineering.* New York: Wiley-Interscience, 667 pp.

McCown, R. L., Jones, R. K., Peake, D. C., 1980: Evaluation of a no-till, tropical legume ley-farming strategy. In: Muchow, R. C., (ed.) *Agro-research for the Semi-arid*

Tropics: Northwest Australia. St. Lucia: University of Queensland Press, pp. 450–469.

Philip, J., de Vries, D. A., 1957: Moisture movement in porous materials under temperature gradients. *Eos Trans. AGU*, **38**, 222–232.

Radke, J. K., 1982: Managing early season soil temperatures in the northern corn belt using configured soil surfaces and mulches. *Soil Sci. Soc. Amer. J.*, **46**, 1067–1071.

Ross, P. J., Williams, J., McCown, R. L., 1985: Soil temperature and the energy balance of vegetative mulch in the semi-arid tropics II Dynamic Analysis of the total energy balance. *Aust. J. Soil Res.*, **23**, 515–532.

Saxton, K. E., Bristow, K. L., Flerchinger, G., Omar, M., 1988: Tillage and crop residue management for water conservation. In: Unger, P. W., Sneed, T. V., Jordan, W. R., Jensen, R. (eds.) *Challenges in Dryland Agriculture – A Global Perspective.* College Station: Texas Agricultural Experiment Station, pp. 494–496.

Shen, Y., Tanner, C. B., 1990: Radiative and conductive transport of heat through flail-chopped corn residue. *Soil Sci. Soc. Amer. J.*, **54**, 653–658.

Tanner, C. B., Shen, Y., 1990a: Solar radiation transmittance of fail-chopped corn residue layers. *Soil Sci. Soc. Amer. J.*, **54**, 650–652.

Tanner, C. B., Shen, Y., 1990b: Water vapor transport through a flail-chopped corn residue. *Soil Sci. Soc. Amer. J.*, **54**, 945–951.

Unger, P. W., Parker, J. J., 1976: Evaporation reduction from soil with wheat, sorghum, and cotton residues. *Soil Sci. Soc. Amer. J.*, **40**, 938–942.

van Bavel, C. H. M., Hillel, D. L., 1976: Calculating potential and actual evaporation from a bare soil surface by simulation of concurrent flow of water and heat. *Agric. Meteor.*, **17**, 453–476.

van Genuchten, M. T., 1980: A closed-form equation for predicting the hydraulic conductivity of unsaturated soils. *Soil. Sci. Soc. Amer. J.*, **44**, 892–898.

Williams, J., Ross, P. J., Bristow, K. L., 1991: Perspicacity, precision and pragmatism in modeling crop water supply. In: Muchow, R. C., Bellamy, J. A. (eds.) *Climatic Risk in Crop Production Models and Management for the Semiarid Tropics and Subtropics.* Wallingford: C.A.B. International, pp. 73–96.

Authors' addresses: K. L. Bristow, CSIRO Division of Soils, PMB, PO Aitkenvale, Townsville, Queensland 4814, Australia; R. Horton, Department of Agronomy, Iowa State University, Ames, IA 50011, U.S.A.

Verleger: Springer-Verlag KG, Sachsenplatz 4–6, A-1201 Wien. — Herausgeber: Prof. Dr. H. Graßl, Joint Planning Staff for the World Climate Research Programme, c/o WMO, Case Postale 2300, CH-1211 Genf 2. — Redaktion: Josef Baumann-Gasse 1, A-1210 Wien. — Satz und Umbruch: Thomson Press (India) Ltd., New Delhi. — Druck und Bindung: Druckhaus Grasl, A-2540 Bad Vöslau. — Verlagsort: Wien. — Herstellungsort: Bad Vöslau. — Printed in Austria.